High Accuracy Digital Quadrature Demodulation

R. J. Inkol
Defence Research Establishment Ottawa
Ottawa, Ontario
Canada, K1A 0Z4

M. Herzig
University of Waterloo
Waterloo, Ontario
Canada, N2L 3G1

R. Saper
Vantage Point International
Gloucester, Ontario
Canada, K1B 5C8

Abstract

The accuracy of digital quadrature demodulation can be improved by optimizing the matching of the inphase and quadrature channel frequency responses. It is shown that an image rejection performance exceeding 100 dB can be achieved using Finite Impulse Response filters having as few as eleven nonzero coefficients.

Introduction

In coherent radar, communication and electronic warfare systems, it is often useful to form the inphase (I) and quadrature (Q) components of a bandpass signal after it has been shifted to a convenient intermediate frequency (IF). The classical analog quadrature demodulation appproach has the problem that accurate amplitude and phase matching of the inphase and quadrature channels cannot be easily achieved [1]-[3]. Another error results from DC offsets introduced during the analog-to-digital conversion of the I and Q signals. These errors are particularly serious in coherent radar systems where they yield spurious sidebands at the image doppler frequency [2]. Consequently, digital approaches for performing quadrature demodulation on a digitized IF signal have attracted attention. Problems with the matching of analog components are eliminated and it is straightforward to achieve high accuracy through the use of filters having a sufficiently large number of coefficients. However, the computational cost can be a significant disadvantage when wideband signals must be processed in real-time.

This problem has led to the development of digital quadrature demodulation algorithms designed for low computational cost [4]-[6]. These also have significant deficiencies. Approaches based on Hilbert Transformers (e.g., [6]) don't suppress DC offsets and require selective analog IF filters since the quadrature demodulator does not have usable stopbands. Alternatively, if Infinite Impulse Response filters are used, as proposed in [5], there are difficulties with a frequency dependent group delay.

Figure 1 shows an alternative digital quadrature demodulator which employs a pair of Finite Impulse Response (FIR) highpass filters whose phase shifts differ by $\pi/2$. The even and odd samples of a bandpass signal nominally centered on an Intermediate Frequency (IF) of f_{IF} and sampled at a rate $f_s=4f_{IF}$ are separately processed by the two filters. The decimation operations reduce the output data rate in each channel to $f_s/4$ and result in the highpass output signals from the filters aliasing to baseband without explicit mixing. The inphase and quadrature highpass filters are obtained by multiplying the coefficients $\{h_{-K}, ..., h_{-2}, h_{-1}, h_0, h_1, h_2, ..., h_K\}$ of a prototype FIR lowpass filter by $\cos k\pi/2$ (even k) and $\sin k\pi/2$ (odd k) respectively. This algorithm is efficient since the inphase filter can be a half-band filter with nearly half of its coefficients equal to zero and the decimation operations result in the output data rate being matched to the bandwidth of the filters. Note that the stopbands of $[DC,f_s/8]$ and $[3f_s/8,f_s/2]$ possessed by the resultant complex filter relax the stopband attenuation requirements of the analog IF filter and suppress DC offsets. The relationship of this quadrature demodulator to approaches involving quadrature mixing and lowpass filtering is discussed in [6].

Although the inphase and quadrature filters are derived from a common prototype filter, they have a different number of coefficients and their frequency responses do not exactly match. The matching of the frequency responses is very important because it determines the phase error/image suppression performance that is obtainable [2].

This paper presents a new approach where the problem of matching the frequency responses is considered in the filter design methodology. It is shown that the error performance is strongly dependent on the choice of filter design parameters and tradeoffs with other performance parameters such as passband flatness are discussed. The results presented are for the window design method, but we have found that analogous results are obtained for the Remez exchange method.

TH 3F

Effects of Filter Design Parameters

The windows considered were the common first and second order cosine windows and the Kaiser and Chebyshev windows. For each window, pairs of I and Q filters having odd numbers of coefficients up to a maximum of 49 were designed. The frequency responses of the filters were determined at 64 discrete frequencies distributed over the bandwidth $[f_s/8,f_s/4]$. Because the frequency responses are symmetric about $f_s/4$, it is not necessary to compute them over the full bandwidth $[f_s/8,3f_s/8]$. The phase error bound [7]

CH3577-4/95/0000-1351$01.00 © 1995 British Crown Copyright

was computed using

$$\phi_e(f_i)=\arctan(|Q(f_i)|/|I(f_i)|)-\pi/4, \qquad (1)$$

where $Q(f_i)$ and $I(f_i)$ are the magnitudes of the frequency responses of the Q and I channels at a discrete frequency f_i. In the time domain, the phase error will oscillate between $-\phi_e(f_i)$ and $+\phi_e(f_i)$ with a frequency $4|f_i-f_s/4|$. For small values of $\phi_e(f_i)$, the RMS value of the phase error at f_i, $\phi_{rms}(f_i)$, will be approximately $\phi_e(f_i)/\sqrt{2}$. Using this result, a measure of the performance for all f_i is provided by the RMS phase error given by $[\Sigma\phi_{rms}(f_i)^2/I]^{-5}$ where I is the number of discrete frequencies. Although this approach is an indirect way of measuring the phase error, we have found good agreement with direct measurements of the phase error of the quadrature demodulator for simulated sinusoidal signals.

Figures 2 and 3 plot the RMS and peak phase errors for the rectangular and common cosine windows as a function of the total number of filter coefficients used by the I and Q filters. The Hamming window, although better than a rectangular window, has a poor performance and its general trend shows only a slow improvement with an increasing number of filter coefficients. The phase error for the Hanning window is considerably better and its trend with respect to the number of coefficients shows a steeper slope. The Blackman window shows a further improvement. A rather different behaviour is observed for the Kaiser and Chebyschev windows plotted in Figures 4 and 5. The phase error rapidly decreases as the number of filter coefficients increases and then fluctuates around a value that is largely determined by the window parameters R and B and has only a weak dependence on the number of filter coefficients.

Another performance parameter that can be measured is the image rejection ratio. For a sinusoidal input signal, the expected output signal of a quadrature demodulator has a spectral component at a frequency corresponding to the frequency offset of the input signal from the center frequency of the quadrature demodulator (f_{IF}). The ratio of the power in this spectral component to the spurious image at the negative frequency is the image rejection ratio. Table I presents image rejection ratios obtained for several filter designs at several frequency offsets.

Some investigations were carried out concerning the effects of different windows on the distortion performance achieved with the quadrature demodulator when used in an FM demodulator. Table II gives the peak spurious signal and total distortion to signal power ratios for the demodulated signal where the input signal is frequency modulated by a sinusoid of frequency $0.00195f_s$ with a frequency deviation of $0.01f_s$.

Discussion and Conclusions

The phase error for a given number of filter coefficients can vary by 5 orders of magnitude depending on the choice of filter window. With a suitable choice of window, it is apparent that very low phase errors can be achieved with relatively low order filters. For example, an RMS phase error of 0.0006 degrees can be obtained with 29 filter coefficients with a Kaiser window having B=7. This is less than the phase error resulting from the quantization of noiseless signal data to 14 bit resolution.

Some generalizations can be made concerning the shape of the windows. Although windows which have low sidelobe levels are usually good, the converse is not always true. For example the Hanning window has a considerably superior phase error/image rejection ratio performance to the Hamming window although having a larger first sidelobe level. The Hanning window also compares well with the Kaiser window having the same mainlobe width (B=5.44) except for filters having a small number of coefficients. However, the Kaiser window, unlike the Hamming window, has a large superiority in passband flatness. In general, the best performance is obtained for windows whose first derivative smoothly decreases to zero at the sample points immediately outside the window bounds. It is not sufficient that the window continuously decrease to zero as is shown by the poor performance of the Bartlett (triangular) window.

The image rejection ratio shows a dependence on the mismatching of the frequency responses of the I and Q channels consistent with the theoretical relationship given by

$$I_r(f_i)= 10Log\frac{1+2E(f_i)+E(f_i)^2}{1-2E(f_i)+E(f_i)^2}, \qquad (2)$$

where $E(f_i)$ is the ratio of gains of the I and Q channels at a frequency f_i and the filters have a relative phase shift of $\pi/2$ [2]. As is the case for the phase error, there is a large variation for different types of windows. It is noteworthy that greater than 100 dB of image suppression can be obtained with only 13 filter coefficients, of which 2 have values of zero.

While very good results can be achieved for the phase error and image rejection ratio with a small number of filter coefficients (for example by using Kaiser or Chebyschev windows with high values of B or R, respectively), there is a high cost in the passband flatness and the size of the transition bandwidth between the pass and stopbands. Since the phase error and image rejection ratio results are for sinusoidal signals at a single frequency, there is no aliasing distortion and deviations from a flat passband frequency response are unimportant. Consequently, it is expected that the errors for wideband signals are much larger, and the flatness of the passband frequency response should be considered in designing the quadrature demodulation filters. Also, the effects of quantizing the filter coefficients can be important in hardware implementations designed for low cost. Nevertheless, quadrature demodulation filters designed for good frequency matching can provide significant benefits in applications such as frequency demodulators for signals having wideband FM modulation providing a sufficiently high sampling rate is used.

References

[1] D.L. Sharpin, J. B.Y. Tsui, J. Hedge, and B. Haber, "The Effects of Quadrature Sampling Imbalances on a Phase Difference Analysis Technique," 1990 National Aerospace Electronics Conference, May 1990.

[2] A. I. Sinsky and P. C. Wang, "Error Analysis of a Quadrature Coherent Detector Processor, "IEEE Trans. on Aerospace and Electronic Systems, AES-10, Nov. 1974.

[3] R. L. Mitchel, "Creating Complex Signal Samples from a Bandlimited Real Signal," IEEE Trans. on Aerospace and Electronic Systems, AES-25, May 1989.

[4] C. M. Rader, "A Simple Method for Sampling In-phase and Quadrature Components," IEEE Trans. on Aerospace and Electronic Systems, VOL. 20, NO. 6, Nov. 1984.

[5] W. M. Waters and B. R. Jarret, "Baseband Signal Sampling and Coherent Detection,", IEEE Trans. on Aerospace and Electronic Systems, AES-18, Nov. 1982.

[6] G. Zhang, D. Al-Khalili, R. Inkol and R. Saper, "Novel Approach to the Design of I/Q Demodulation Filters," IEE Proc.-Vis. Image Signal Processing, Vol. 141, No. 3, June 1994.

[7] J.Lee, "Effects of Imbalances and DC offsets on I/Q Demodulators," DREO Report No. 1148, Dec. 1992.

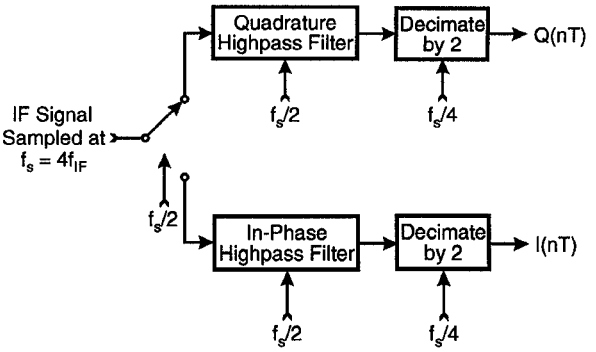

Figure 1. Quadrature demodulation algorithm. The IF center frequency f_{IF} and Nyquist bandwidth are fixed at $f_s/4$.

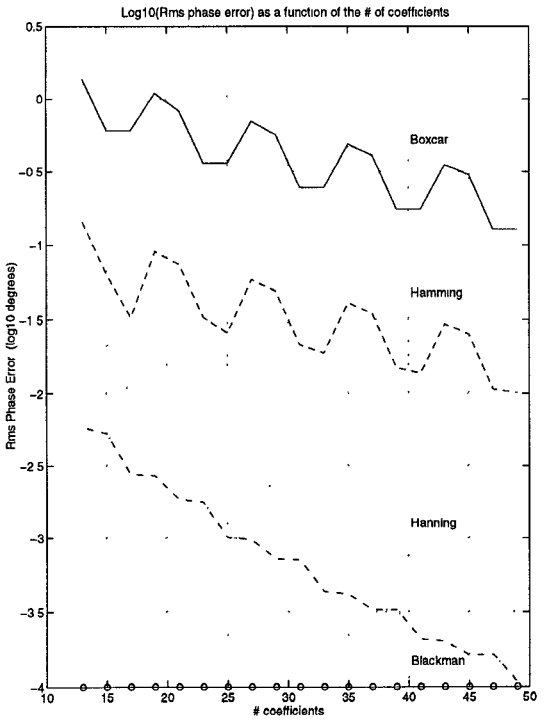

Figure 2. RMS phase error over $[f_s/8, 3f_s/8]$ for rectangular and cosine windows as a function of the total number of filter coefficients.

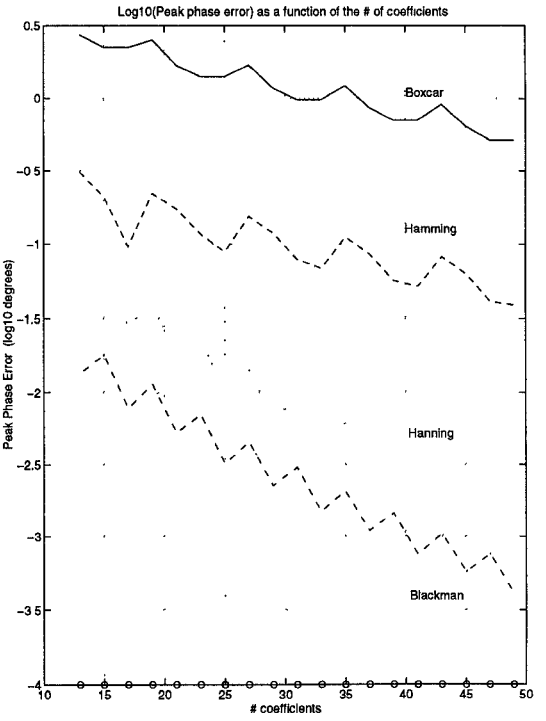

Figure 3. Peak phase error over $[f_s/8, 3f_s/8]$ for rectangular and cosine windows as a function of the total number of filter coefficients.

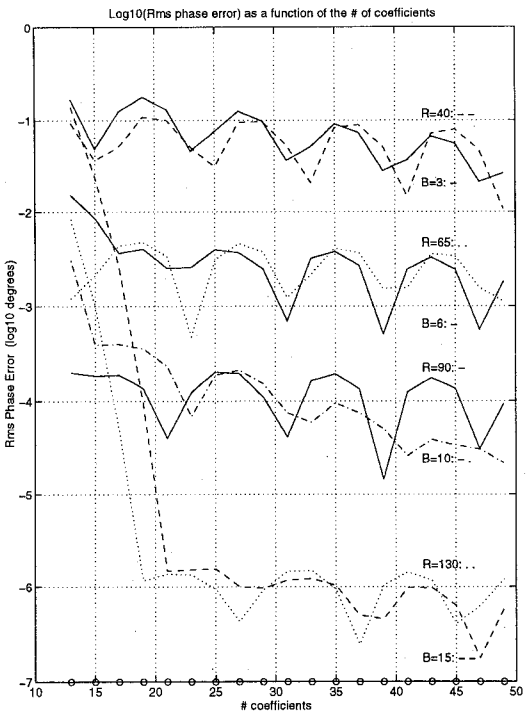

Figure 4. RMS phase error over $[f_s/8,3f_s/8]$ for Kaiser and Chebyshev windows as a function of the total number of filter coefficients.

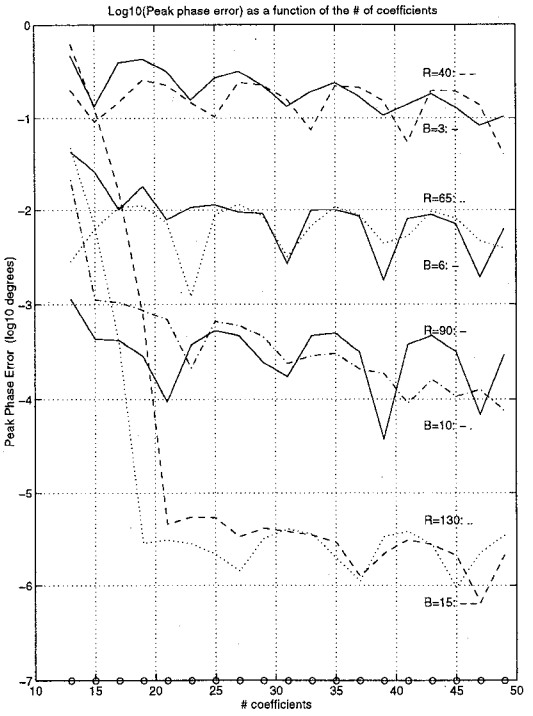

Figure 5. Peak phase error for Kaiser and Chebyshev windows over $[f_s/8,3f_s/8]$ as a function of the total number of filter coefficients.

	F_{off} = ±0.00195	F_{off} = ±0.125	F_{off} = ±0.25	F_{off} = ±0.375
Hamming (N=13)	47.8 dB	56.9 dB	48.8 dB	45.7 dB
Hanning (N=13)	66.4 dB	73.5 dB	65.6 dB	59.7 dB
Cheb. (N=13, R=90)	108.1 dB	115.4 dB	109.0 dB	104.1 dB
Hamming (N=29)	56.3 dB	56.6 dB	57.6 dB	58.5 dB
Hanning (N=29)	88.0 dB	88.2 dB	88.9 dB	89.6 dB
Cheb (N=29, R=200)	141.6 dB	142.1 dB	143.3 dB	145.1 dB

Table I. Image rejection ratio for sinusoidal signal offset in frequency from quadrature demodulator center frequency. Frequency offsets are normalized to -0.5 at $f_s/8$ and +0.5 at $3f_s/8$.

Number of Coeff.	Hamming	Hanning	Chebyshev
13	47.3 dB (44.8 dB)	65.8 dB (63.3 dB)	107.6 dB (105.1 dB) (R=90)
29	55.9 dB (53.4 dB)	87.6 dB (85.1 dB)	141.1 dB (138.3 dB) (R=200)
45	58.8 dB (56.3 dB)	115.6 dB (113.1 dB)	141.1 dB (138.3 dB) (R=200)

Table II. Peak Spurious Signal and, between parenthesis, Signal to Distortion Ratio for demodulated signal having sinusoidal frequency modulation (Fexc = $0.01f_N$, Fmod = 0.00195 f_N, $f_N = f_s/4$). FM demodulation is performed by differentiating the unwrapped signal phase using a 5 point Lagrange differentiator.